**Serb. Astron. J. № 170 (2005), 1 - 12** **UDC 521.1 : 523.31**
Invited review

# THE EARTH ORBITING SPACE DEBRIS

**A. Rossi**

*ISTI–CNR*
*Via Moruzzi 1, 56124 Pisa, Italy*

(Received: April 15, 2005; Accepted: April 15, 2005)

**SUMMARY: The space debris population is similar to the asteroid belt, since it is subject to a process of high-velocity mutual collisions that affects the long-term evolution of its size distribution. Presently, more than 10 000 artificial debris particles with diameters larger than 10 cm (and more than 300 000 with diameters larger than 1 cm) are orbiting the Earth, and are monitored and studied by a large network of sensors around the Earth. Many objects of different kind compose the space debris population, produced by different source mechanisms ranging from high energy fragmentation of large spacecraft to slow diffusion of liquid metal. The impact against a space debris is a serious risk that every spacecraft must face now and it can be evaluated with ad-hoc algorithms. The long term evolution of the whole debris population is studied with computer models allowing the simulation of all the known source and sink mechanisms. One of these codes is described in this paper and the evolution of the debris environment over the next 100 years, under different traffic scenarios, is shown, pointing out the possible measures to mitigate the growth of the orbital debris population.**

**Key words. Earth – Celestial mechanics**

## 1. INTRODUCTION

Long time ago, in the early history of the human race, the mankind was facing almost virgin environments: the sea, the forests, the meadows, untouched remote islands,.... One after another, all these environments have been altered, exploited and polluted. By the middle of last century, there existed perhaps one single environment near us that had remained virgin and unexploited: the space. Then, the first artificial satellite, Sputnik 1, was launched by the USSR on October 4, 1957. A few years later, on June 29, 1961 the first known break–up in orbit, the explosion of the *Transit 4A* rocket body took place. From then on, the repetition of these two events (launches of new satellites and break-up of spacecraft in orbit) contributed to build up a huge population of objects that are now polluting, perhaps in an irreversible way, the space around us. These objects, the space debris, now jeopardize all the human activities in space. On July 24, 1996, merely 40 years after the first man-made object ever entered the space above the planet, the first recorded accidental collision between an operational satellite and a piece of debris was recorded: the French microsatellite *Cerise* was hit, at the relative velocity of 14.77 km/s, by a fragment of about 10 $cm^2$ coming from the explosion of an Ariane rocket upper stage, oscurring ten years before (Alby et al. 1997). All of a sudden, collisions with space debris became a reality. Though still very unlikely from a statistical point of view, collisions are going to become the most important source of debris in a not too distant future and a nightmare for all the space missions, especially the manned ones. In this paper I will try to describe and analyze how the overcrowding of the circumterrestrial space became possible, how are the space debris observed and detected, what are the space debris

and where they are, what danger they pose to other orbiting facilities, what is going to be the future evolution of the space environment and, finally, what we are trying to do in order to mitigate, if not eliminate, the problem.

## 2. OBSERVATION OF SPACE DEBRIS

All the un-classified spacecraft currently in orbit are cataloged by the United States Space Command in the Two–Line Element (TLE) catalog. In this catalog about 10 000 objects are listed along with their current orbital parameters. The limiting size of the objects included in the catalog (due to limitations in sensors power and in observation and data processing procedures) is about 5 to 10 cm below a few thousands km of altitude and about 0.5 - 1 m in higher orbits (up to the geostationary ones). The orbits of the TLE catalog objects are maintained thanks to the observations performed by the Space Surveillance Network (SSN). The network is composed of 25 sensors, both radars and optical sensors. The radars include mechanically steered dishes, one radar interferometer (the NAVSPASUR "radar fence", composed of a network of three transmitting and six receiving radar sites spanning the continental US along the $32^{nd}$–$33^{rd}$ parallel) and large phased–array radars capable of tracking several objects simultaneously. These latter radars can track objects from just above the horizon to just short of the zenith over an azimuth of 120 degrees. Capable of generating more than 30 megawatts of radio frequency power, they can track space objects in excess of 40 000 km in range and represent the largest source of information for the catalog, especially in Low and Medium Earth Orbit. The recent introduction of the large L-band "Cobra Dane" radar in Alaska, for example, raised the number of objects in the catalog by about 10 % pushing the network to its limits in terms of processing and archiving power, to the point that, at present, the principal limitation to the cataloging capabilities seems to be exactly the processed structure and not the sensors power.

Above several thousand km of altitude, the radar power is not sufficient to monitor the small space debris, as the returned flux is proportional to the $-4$ power of the distance, and the SSN uses optical sensors for the higher objects. Until 1987 the well–known Baker–Nunn photographic systems were the primary sources for optical information; they had a limiting magnitude of 14 and used photographic plates, which required long processing. Therefore, after 1987 they were replaced by electro–optical devices, which embrace the Ground-based Electro-Optical Deep Space Surveillance System (GEODSS), including 6 different observing sites. This system, combining three telescopes (two primary 1 m telescopes and one 40 cm auxiliary) in each observing site, achieves accurate pointing and a very good sensitivity (limiting magnitude about 16.5). Tracking and data processing is now automated and about 80 000 observations are processed daily by the SSN.

To get data on the smaller objects in Low Earth Orbit (LEO) not included in the catalog, different sensors, or the same sensors but operated in a different way, are needed. Radar campaigns have been carried out to detect objects of 1 cm and below by putting the radar in a "beam park" mode, where the radar stares in a fixed direction and the debris randomly passing through the field of view are detected. This allows a counting of the number of objects, i.e., the determination of the objects flux and density, but only a rough determination of their orbits.

As far as the geostationary ring is concerned, dedicated, non-routine, optical observation campaigns have been performed to characterize the environment in this vital region of the circumterrestrial space. In particular, until a few years ago, NASA used the liquid mirror telescope installed in Cloudcroft, New Mexico, USA. Now dismissed, it was a 3 m diameter parabolic dish holding four gallons of liquid mercury and was specifically devoted to space debris observations in the GEO region. The European Space Agency has installed, for this purpose, a 1 m Schmidt telescope in the Canary Islands, now fully operating and providing an abundance of new data. The limiting detection size in GEO for this telescope is about 20 – 30 cm. It is just the case to mention here that of course space debris are routinely "observed" also by astronomers worldwide, that find their plates polluted by the tracks of the unwanted objects passing through the observation field.

The ground based observations are then supplemented by the data, mainly about mm and sub-mm particles, obtained from the analysis of the surfaces of spacecraft returned to Earth after some time spent in orbit (e.g. the Long Duration Exposure Facility (LDEF), a satellite released and then retrieved by the Space Shuttle, the Hubble Space Telescope solar panels, the Space Shuttle external surface itself, etc) and from impact sensors on board a few satellites.

## 3. THE SPACE DEBRIS POPULATIONS

The ground observations and in-situ data allow to calibrate the models of the space environment describing the nature and the location of the space debris. There are models produced mainly by fitting the observational data to derive values of the flux of debris as a function of the altitude and on a given orbit (Liou et al. 2002). Another kind of models reconstruct the environment by reproducing all the known source and sink mechanisms (see Section 5) with ad-hoc computer models. One of these latter models has been developed by the European Space Agency and is called MASTER 2001 (Klinkrad et al. 2004). Figs. 1 – 3 have been produced by using the MASTER 2001 population of objects.

Only about 6% of the objects in the TLE catalog are operative satellites. Approximately 24% is composed by non-operative spacecraft; around 17% by the upper stages of the rockets used to place the

satellite in orbit. In fact, about 5 000 payloads have been launched since the Sputnik I. Among these objects, some 3 000 have re–entered in the atmosphere. The others (about 2 000) are still orbiting and represent the majority of the large ($> 1$ m) objects in orbit. About 13% consist of mission related debris (e.g., sensors caps, yo-yo masses used to slow down the spacecraft spin, etc). Finally some 40% are debris generated mostly by about 170 explosions and 2 collisions which have involved rocket upper stages or spacecraft in orbit (Klinkrad et al. 2004). About 99% of the mass in orbit is due to the large objects included in the catalog.

The population of objects smaller than several centimeters is statistically known thanks mainly to sporadic radar campaigns. Whereas the fragmentation debris were thought to be the only small particles present in space until about 10 years ago, the radar and in-situ measurements brought to light a series of new unexpected populations of debris. The observation campaigns performed with the Haystack radar, located near Boston in the US, led to the discovery of a large family of objects determining a prominent peak of density of objects around 900 km of altitude (see Fig. 1). This density peak is mainly due to the presence, in this altitude band, of a large number of sodium-potassium liquid metal droplets leaked from the Russian ocean surveillance satellites (RORSAT) (Foster et al. 2003). This liquid was used as a coolant for the nuclear reactor which generated the power on board and was dispersed in space after the core of the reactor was ejected from the spacecraft in order to prevent possible risks due to its reentry into the Earth atmosphere. About 70 000 drops with diameter between 0.5 mm and about 5.5 cm have been estimated to orbit the observed region.

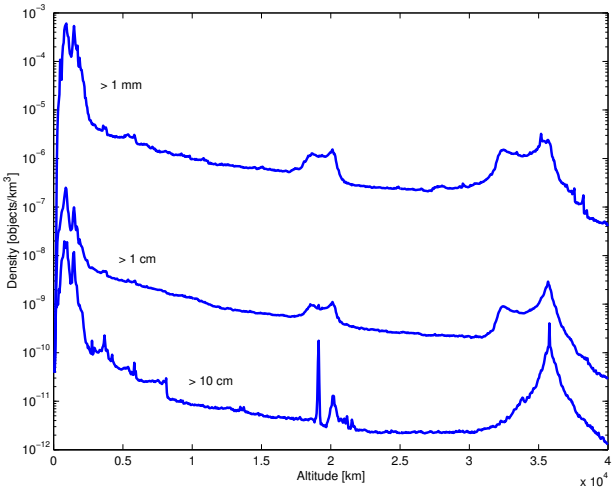


**Fig. 1.** *Density of objects as a function of altitude for three different size thresholds: objects with diameter larger than 1 mm, 1 cm and 10 cm.*

Another previously unknown debris population, at around 2900 km of altitude, consisting of the so-called *West Ford Needles* has been detected by radar surveys. Using the powerful Goldstone radar, Goldstein et al. (1998) found the remnants of the copper dipoles, 1.77 cm long, which were released in space in 1961 and 1963 by the American satellites Midas 3 and Midas 6, for telecommunication experiments. They were conceived to reenter the atmosphere in about 5 years, but apparently some of them stuck together after the release, lowering thus their area over mass ratio and, therefore, augmenting their orbital lifetime. According to the Goldstone observations, a population of about 40 000 such clusters is orbiting between 2400 and 3100 km of altitude.

The Haystack observations were instrumental also to point out the importance of another unexpected source of space debris, the aluminum oxide ($Al_2O_3$) particles coming from the burns of the rocket motors with solid propellant. During these burns a large number of sub-millimeter sized particles are ejected. As a matter of fact the solid rocket motor (SRM) exhausts are probably the main contributors to the debris population between 10 $\mu$ and 100 $\mu$. Between 100 $\mu$ and 1 cm the SRM exhausts are again one of the main components of the population, together with fragments and paint flakes detached from spacecraft surfaces exposed to the space environment effects. In some cases (particularly toward the end of the burn) also slugs of this propellant are released from the SRM, which are of centimetric dimensions (Jackson et al. 1997); particularly at low inclinations, where the SRM firings have been more frequent, these slags particles could be responsible for a significant portion of the centimetric debris and even dominate the 1 cm population below about 400 km and above 2 500 km of altitude (see Section 4).

The current estimate, derived from the observations and the simulated populations, is that the total number of non–trackable particles of 1 cm and greater is around 350 000, while those larger than 1 mm could be more than $3 \times 10^8$.

Fig. 1 shows the density of objects for three different size regimes as a function of altitude and highlight the three main zones of accumulation in space: the region of the Low Earth Orbits (LEO, below about 2000 km), the Medium Earth Orbits (MEO, between 2000 km and about 36 000 km) and the Geostationary Orbits (GEO, above 36 000 km).

To find out the distribution of the objects within these large regions it is useful to look at the plots with respect to the position of the objects in the orbital elements space. In Fig. 2 the cataloged objects are plotted in the semi-major axis versus inclination space. This representation clearly highlights some features in the distribution of objects with the spacecraft (and the resulting debris) being clearly grouped in "families" or constellations, according to their different purposes and to the different launching bases.

In LEO, we can distinguish the satellites in Sun-synchronous orbits ($i \simeq 100°$), the satellites in polar orbits ($i \simeq 90°$), some families of Russian COSMOS satellites between $i \simeq 60°$ and $i \simeq 80°$, the LEO satellites launched from the Kennedy Space Center (at $i \simeq 27°$). In MEO, we see the Russian communication satellites in Molniya–type orbits ($a \simeq 26,000$ km, $e \simeq 0.7$, $i \simeq 63°$), the families of

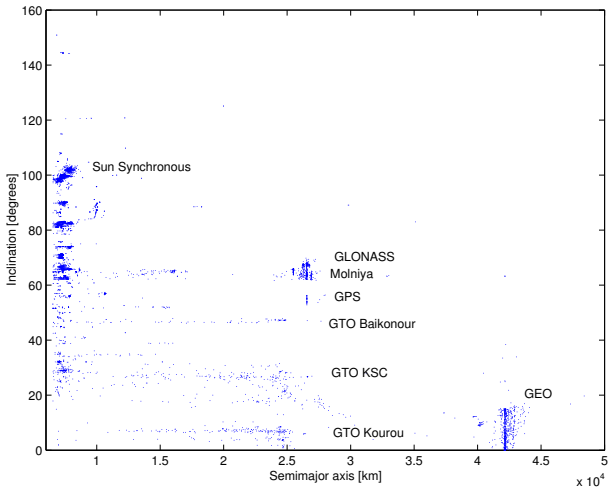


**Fig. 2.** *Distribution in the semimajor axis - inclination space of the objects included in the TLE Catalog.*

objects in geosynchronous transfer orbits (GTO) (mostly upper stages) launched from Kourou (ESA Ariane rockets, $i \simeq 7°$), from the Kennedy Space Center ($i \simeq 27°$) and from Baikonour ($i \simeq 48°$) and the US GPS (Global Positioning System) satellites and their Russian analogues GLONASS ($a \simeq 26,000$ km, $i \simeq 55°$ and $i \simeq 63°$, respectively). The GPS and the GLONASS are the two currently deployed navigation constellations. Along with the Russian telecommunication spacecraft in Molnyia orbits, they are the most sensible objects orbiting the MEO region. According to the MASTER 2001 population model, in the MEO region there are about 60 000 objects larger than 1 cm that are possibly crossing the orbits of the navigation constellations. Actually most of the objects in MEO are clustered about the Molnyia orbits and have therefore a minimal interaction with the navigation constellations. But, even if we exclude the objects close to Molnyia orbits, about 16 000 objects with diameter larger than 1 cm have orbits potentially crossing the navigation constellations. In particular, the GPS orbit appears within reach of several thousand objects, due to the non-zero eccentricity of most of the debris in the MEO zone. The risk of an impact in this region and its possible consequences on the navigation constellations is discussed in Section 4.

Finally, in Fig. 2 we note the geosynchronous satellites ($a \simeq 42,000$ km, $e \simeq 0$, $15° \geq i \geq 0°$). Notwithstanding its paramount importance, the picture of the debris environment in the GEO region is still very uncertain, mainly due to the physical distance which prevents its mapping by radars. The peculiarities of the GEO region are mainly the absence of any natural decay mechanism, such as air drag (see Section 5) and the fact that each satellite in geostationary orbit is assigned an "orbital slot" of about 0.1° of width in longitude. For these reasons, though huge in physical terms, the useful space in the GEO region is actually operationally limited since an orbital slot not freed by a "dead" satellite (or a debris) is not any more usable by other spacecraft. Moreover any debris created in the region will stay there almost for ever. Note that, during their operative lifetime, the satellites are periodically maneuvered to keep them inside the slot, counteracting the perturbations that would tend to change their orbital parameters. In particular perturbations due to the Sun, the Moon and the Earth oblateness would induce a precessional motion of the orbital plane inclination, inducing an 15° oscillation of $i$, with a period of about 53 years. Also, the solar radiation pressure would induce small periodic variations in $e$. Therefore, once the satellite is no more operational its inclination and eccentricity will tend to deviate from the nominal zero values. This means that they will start crossing the operational orbits with relative velocities of several hundreds m/s, much higher than those common for operative co-orbiting GEO satellites. Dedicated optical observation campaigns are performed to characterize the environment in this orbital region. The observations performed since 1999 lead to unexpected and worrying results (Flury et al. 2000, Schildknecht 2004). About 1040 objects have been detected near GEO. Only 340 are active satellites, while the rest are debris, mostly uncatalogued objects. The source of this objects remains still uncertain since only two explosions have been recorded in GEO and these two events cannot account for all the observed debris. Probably ten more unrecorded fragmentation events must have happened in GEO (Klinkrad et al. 2004). Of course the number of non-trackable objects, smaller than the telescope detection threshold, should be much larger than 1000. A large uncertainty remains in the geostationary region and international efforts are under way to improve our knowledge in this area.

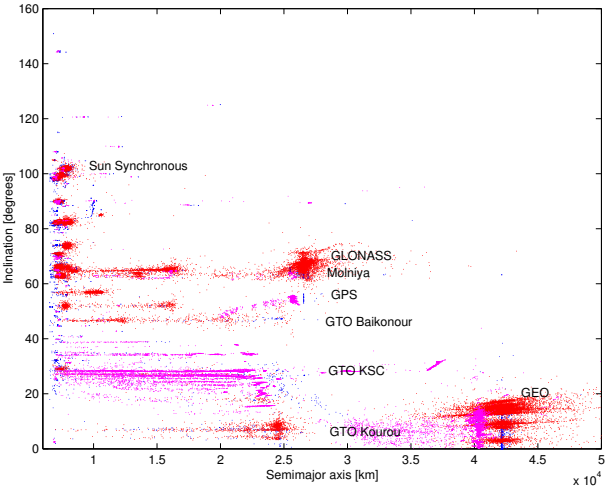


**Fig. 3.** *Distribution in the semimajor axis - inclination space of the objects larger than 1 cm.*

Fig. 3 shows the distribution of the objects larger than 1 cm from the MASTER 2001 population. The families of orbits, described in Fig. 2, are still recognizable. Nonetheless, they are now covered

by large clouds of smaller objects. Note the spread of the orbital elements (mostly in semi-major axis, since it is very expensive to impart changes in inclination) due to the energy imparted to the fragments in case of breakups. The long stripes of objects at the inclination of the different GTOs are mainly due to the release of the slag by the SRM of the upper stages. Also noticeable, with respect to the situation in the 10 cm size range, is the large number of objects in the GEO vicinity due both to slag from upper stage burns and to the large number of uncatalogued fragments.

## 4. COLLISION RISK

The overcrowding of the space around the Earth makes collisions a serious threat and, as pointed out by the *Cerise* event, a reality. To protect the space assets against impacts with small debris ($\leq$ 1 cm) multi-wall bumper shields have been devised and installed on some modules of the International Space Station (ISS). Yet, for larger debris the shields are not enough to prevent the penetration of the target or even its complete fragmentation; in this case an avoidance maneuver, if the projectile is

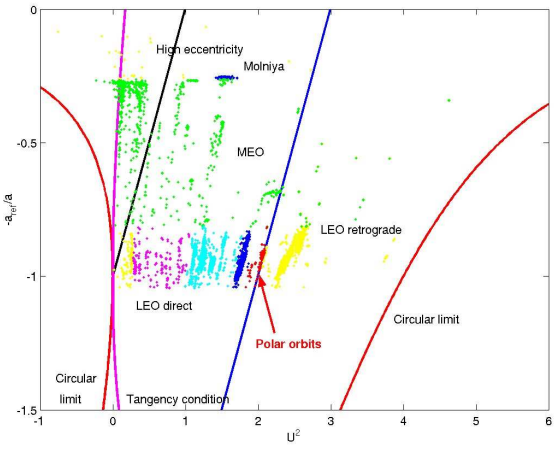


**Fig. 4.** *Representation of the TLE catalog population in the space $U^2$ vs $E = -a_{\rm ref}/a_{\rm projectile}$, for a target in a circular equatorial ($i = 0°$)orbit, at 450 km of altitude. For a thorough explanation of the lines drawn in the plot, refer to Valsecchi et al. (1999). Note that the admissible region is included between the two circular limits and that the objects possibly crossing the orbit of the target lie to the right of the tangency condition. The objects to the right of the inclined line starting from the target position have higher probability of hitting the target on the front; on the left of this line impacts from the back predominate (the more so as we approach the tangency condition). Finally, the straight line from $(1.5, -1.5)$ to $(3, 0)$ is the locus of orbits with inclination equal to 90° with respect to the selected reference plane.*

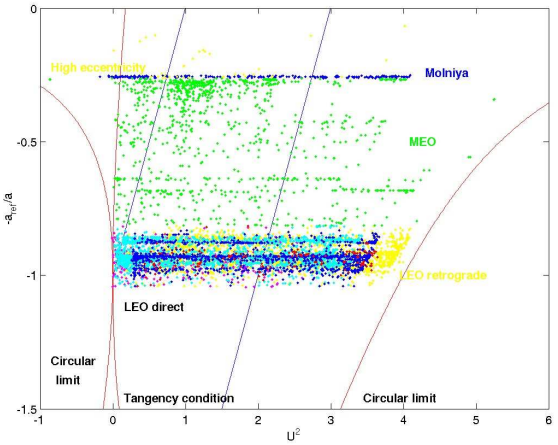


**Fig. 5.** *The same as Fig. 4 for a target orbit with inclination $i = 52°$.*

trackable from the ground, is the only solution to save the Station module. Note however that, as specified in the Section 2, most of the debris between 1 and 10 cm are not cataloged. In addition, most of the operational satellites cannot carry the heavy bumper shields so they can rely only on avoidance maneuvers or on their "good luck" to survive the harsh debris environment. Also the Space Shuttle has already performed several maneuvers to avoid pieces of junk which might have crossed its path.

To highlight the collision risk, another interesting way of representing the space debris population is shown in Figs. 4 and 5, following Valsecchi et al. (1999). This representation is based on Öpik's (1976) studies of the close approaches between small bodies and the planets, and provides useful insight into the dynamics of the overall debris population with respect to a selected target orbit. Öpik's analytical expressions relate in a simple way the semi-major axis $a$, eccentricity $e$ and inclination $i$ of the projectile orbit to the magnitude and direction of the relative velocity vector at impact $\vec{U}$, in a reference frame that is well suited to describe the impact risk for a target in a circular LEO.

In this representation, the space debris population is plotted as a function of the square of the impact velocity, $U^2$ (in units of the target orbital velocity, i.e., about 7 km/s in LEO), of every object with respect to a selected target in a given circular orbit. In Fig. 4 the population of the cataloged objects of Fig. 2, is plotted with respect to a target in an equatorial ($i = 0°$) circular orbit with semi-major axis $a_{\rm ref} = 6\,828$ km. The different families of objects are still recognizable, but now the additional information about the impact velocity against the selected target is available. Moreover, all the objects found on the left of the line tagged "Tangency condition" are not crossing the target orbit, and therefore are not potential projectiles. Note also how, in the same 2-dimensional plot, the information about the eccentricity and the inclination of the projectile or-

bit, with respect to the target one, is included. In Fig. 5 the same population is plotted with respect to a target in a circular orbit with the same $a_{\rm ref}$ but with $i = 52°$ (i.e., an orbit similar to the one of the ISS). Note how the projectile population spreads and mixes and especially how the impact velocities can become significantly larger since the relative inclination between the target and the projectile orbit has to be taken into account. Therefore, also almost head-on collision at very high velocity can take place.

The great advantage of Öpik's approach is that the probability and the geometry of the impacts on a given target can be expressed by means of simple analytical relations. In fact, given a projectile and a target (on a circular orbit of radius $a_0$), the intrinsic collision probability per unit time in Öpik's theory is simply given by (Öpik 1976):

$$P = \frac{U}{2\pi^2 \left(\frac{a}{a_0}\right)^{1.5} |U_x| \sin I} \qquad (1)$$

(we have assumed $\sqrt{GM_\oplus} = 1$) where $U = |\vec{U}|$, $U_x$ is the x-component of $\vec{U}$ (in the frame centered on the target, with the $y$-axis pointing in the direction of the target's instantaneous motion, and the $x$-axis pointing away from the Earth), and $I$ is the inclination of the orbit of the projectile relative to that of the target

Together with the thousands of objects in space there are a few spacecraft that represent particularly sensitive targets for impacts. Between these a fundamental role is played by the ISS due to its large dimensions and to the presence of astronauts on board. By means of the method of Valsecchi et al. (1999) the nature of the impact risk on the ISS was analyzed in greater detail (Valsecchi and Rossi 2002).

In the frame centered on the ISS (with the $x$ and $y$ axis defined as above), two angles can be defined: the colatitude $\theta$, i.e. the angle between $\vec{U}$ and the $y$ axis, and the longitude $\phi$, measured from the $U$-$y$ plane to the $y$-$z$ plane. Analyzing, in this frame, the geometry of the potential impacts on the ISS of all the objects included in the MASTER 99 model of the population of space debris (the precursor of the above mentioned MASTER 2001), we found that the potential impactors tend to come from directions close to the $\sin\phi = 0$ plane, the deviation from this plane being a decreasing function of the impact velocity $U$. Then, most of the objects crossing the ISS orbit have impact velocities between about 9 and 12 km/s, with impact probability in excess of $10^{-10}$ m$^{-2}$ y$^{-1}$. The SRM-related particles dominate the potential impactors (in the MASTER 99 population) for nearly entire velocity range; only at velocities above 13 km/s, the impactor population is dominated by fragments. By coupling the Öpik method analysis and SDM, the long term evolution code described in the next Section, we also calculated the evolution of the impact risk for the next 20 years, taking into account the actual evolution of the altitude profile of the ISS. In fact the ISS will not orbit at a (nearly) constant altitude above the Earth. Instead, its orbit will follow a constant atmospheric density profile. Since the atmospheric density varies periodically with time, according to the varying solar activity, the ISS altitude will vary by about 100 km between 340 and 440 km.

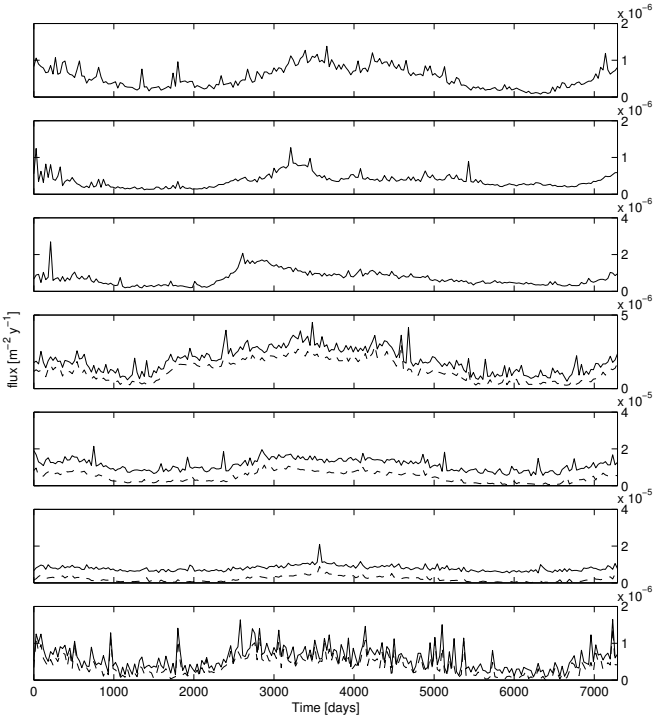


**Fig. 6.** *Debris flux on the ISS in the next 20 years. The solid line is the total flux. In the 4 lowermost plots, the dashed line is the flux due to the SRM related particles. The seven panels show, from bottom to top, the fluxes at increasing impact energies E:* $10^3 < 2E < 10^4$ *J;* $10^4 < 2E < 10^5$ *J;* $10^5 < 2E < 10^6$ *J;* $10^6 < 2E < 10^7$ *J;* $10^7 < 2E < 10^8$ *J;* $10^8 < 2E < 10^9$ *J;* $2E > 10^9$ *J.*

This accounts for a large difference in the impinging flux of debris which translates in large difference in the impact risk. In Fig. 6 the flux level on the ISS for the next 20 years is plotted, divided in ranges of impact energy, from $10^3 < 2E < 10^4$ J in the lowermost panel to $2E > 10^9$ J in the uppermost one. The solid line shows the total flux, while the dashed line represents the flux due only to the SRM particles. It can be noticed that the SRM are the major contributors to the flux at lower impact energies. On the other hand, due to their low masses and, partially, also to their lower impact velocities, the SRM particles do not contribute to the flux for impact energies larger than $10^7$ J. A variation in time by a factor 2 – 3 in the flux, can be noted in most of the impact energy ranges. From the debris flux standpoint, the most critical part of the ISS mission will be the central one when the Station will orbit in the more crowded altitude band around 450 km.

Another set of particularly sensible targets

in space are the multi-plane satellite constellations. The complex interaction between the dynamics of a debris cloud generated by the accidental fragmentation of a constellation spacecraft and the overall dynamics of the satellites in the constellation planes can be effectively studied by the Öpik's method. This interaction is due to the interplay between the collision debris orbital evolution, under the effect of the initial impulse after the break-up and of the geopotential (and the air drag in LEO), and the global precessional motion of the planes of the constellation, under the effect of the Earth's $J_2$. The result is a dangerous collective behavior that can strongly enhance the collision risk within the constellation, with respect to the background flux normally affecting the constellation orbit. We studied different Walker-like LEO constellations (Rossi et al. 1999, Rossi et al. 2001). The largest such constellation currently orbiting is IRIDIUM. It consists of 66 LEO satellites (plus 6 spares) orbiting in 6 different orbital planes at an altitude of about 780 km and with an inclination of 86°.4 to the Earth's equator.

We have found that, in the impact energy range between about $10^7$ and $10^8$ J, corresponding to disruptive projectiles, the collision probability due to the fragmentation debris stays higher than the background level from the general orbiting population for several years. This means that, after the initial break–up, there will be a probability of the order of 10% that a second one will follow within five years, and eventually this may trigger a collisional chain–reaction effect (at the constellation altitude) with a characteristic time scale of about one century, much less than the current estimates with the general debris population (some 300–500 yr; Cordelli et al. 1998).

The same kind of study has been performed for the MEO constellations used for global navigation, namely GPS, GLONASS and the forthcoming European GALILEO (Rossi et al. 2004a). The problem with MEO is that the precession rates of the perigee argument ($\dot{\omega}$) is about two orders of magnitude smaller at the GPS altitude than in LEO ($\dot{\omega}_{\rm GPS} \simeq -0.02$ deg/day). Since a basic assumption of Öpik's theory is that the argument of perigee $\omega$ of the projectile orbit, evaluated using as reference plane the orbital plane of the target, is randomly distributed between 0 and $2\pi$, this slower evolution prevents the direct application of our original method to MEOs. We therefore devised an extension to the method (Valsecchi et al. 1999) to take into account also orbital regimes where the randomization of the angular elements cannot be granted. With this improved method, the collision risk for the navigation constellations, following a fragmentation of a spacecraft, has been analyzed. We studied both the intra-constellation and the inter-constellation risks. Namely, we showed the risk posed by the debris coming from the fragmentation of, e.g., a GPS satellite on the GPS constellation itself and the risk posed by these debris on the other two constellations in the region. The slower dynamics (in terms of precession of the angular arguments of an orbit) of the MEO region prevent the appearance of the strong global effects observed for the LEO constellations. In general terms it has been observed that the flux following a generic fragmentation is by far larger than the low background flux in MEO. The values, spanning the range $10^{-6}$ to $10^{-8}$ m$^{-2}$ yr$^{-1}$ according to the different impact energy levels, still account for low risks in terms of impacts per year. However, the very sensible applications of the navigation constellation call for a high level of reliability that could be seriously endangered by such prolonged levels of debris fluxes. Moreover the strong potential interaction of the three constellations has been highlighted, by displaying the inter-constellation effects of a fragmentation event. In some cases the space distribution of the three systems is such that a larger flux is experienced if the fragmentation event happens in a different constellation.

## 5. THE LONG TERM EVOLUTION

At the end of the '70s, Donald Kessler (Kessler and Cour-Palais 1978) first pointed out the possibility that the process of mutual collisions between the objects presently in orbit could lead to the creation of a debris belt surrounding our planet and jeopardizing, if not preventing, all the space activities. Mathematical models and large numerical codes have been developed to simulate the interplay of all the physical processes involved in the evolution of the debris population. We distinguish source mechanisms, injecting objects in the space, and sink mechanisms, removing objects from the space. The former include: launches, fragmentations (both explosions and collisions) and non-fragmentation events such as Solid Rocket Motor exhausts and the RORSAT drops.

Since the launches are the only source that adds mass to the population in orbit, it is of great importance to be able to predict, in a reliable way, the future space traffic. On the other hand, it is extremely difficult to make a reliable forecast since the traffic will depend on several technical, economical and political factors. The best way to deal with this problem is to produce models able to simulate, in an efficient way, different traffic scenarios and to compare the results of the various cases to identify significant trends.

The fragmentations due to explosions of on-orbit spacecraft represent the major source of cataloged objects. After an explosion, a single object produces a swarm of fragments with a mass distribution that approximately matches exponential laws of the form:

$$N(>m) = N_0\, e^{-c\sqrt{m}}.$$

There are several possible causes for the explosion of a spacecraft. In the past, the most frequent have been deliberate explosions (either to test anti-satellite weapons or to prevent the re-entry in the atmosphere of sensible classified hardware), breakup of abandoned upper stages due to the build up of the pressure of residual propellant left inside the tanks, and battery related explosions. Fortunately, the mitigation measures already implemented (see

Section 5) make the explosions infrequent. In the last five years only about one explosion of a large spacecraft was recorded, on the average, every year.

Although only one accidental collision has been recorded up to now, the collisions are going to represent the most important source of debris for the long term evolution of the space environment. The energy involved in a collision at about 10 km/s (the average impact velocity for orbiting bodies in LEO, is about 9.7 km/s (Rossi and Farinella 1992)) is huge, of the order of $10^3$ Joules even for a centimetric projectile. The mass distribution of the fragments follows a power law:

$$N(> m) \propto m^{-b}$$

where $b$ is a suitable positive exponent ($< 1$ to be consistent with a finite total mass). This mass distribution means that more small fragments are produced in an explosion. In our model, the exponent $b$ has typically an energy-dependent value (Petit and Farinella 1993). If the ratio between the energy of the projectile and the mass of the target is larger than a given threshold $Q^\star$, the target is completely fragmented. Otherwise only a localized damage occurs. The typical value of $Q^\star$ for a spacecraft is about 40 000 J/kg; it is interesting to note that $Q^\star$ is about one order of magnitude larger than the values found for natural bodies, such as asteroids. This is due not only to the difference in material composition, but mostly to the fact that the void structure of a satellite is less efficient in transmitting the impact shock. The few laboratory experiments, with non-classified results, make it very difficult to estimate, in a fully reliable way, the outcome of a hypervelocity collision (i.e. a collision where the impact velocity is larger than the velocity of sound inside the materials, typically around 5 km/s) between space objects. This remains one of the most important uncertainties in modeling the space debris evolution.

As described in Section 3, other non-fragmentation debris sources played an important role in determining the present population of orbiting debris. The SRM slag production can be modeled with a diameter distribution of the form:

$$N(> d) \propto \left(\frac{d^*}{d}\right)^3$$

where $d^*$ is a selected reference diameter derived from radar measurements performed by MIT Lincoln Lab. for a suborbital STAR-37 motor burn. The use of solid rocket motors in space is declining, making this source of objects less important for the long term evolution of the population.

The RORSAT drops, being limited to a specific class of satellites not used any more, should not represent a significant source of debris in the future.

On the other side, there are the sink mechanisms, that is the processes that tend to remove objects from the orbit. The natural perturbations acting on an orbiting spacecraft and altering its motion from a pure two body orbit can be divided in two main classes: gravitational and non-gravitational perturbations. The gravitational perturbations, are due to the non-spherical shape of the Earth and to the presence of a third body (the Moon or the Sun in our case). These perturbations do not affect the semi-major axis of an orbiting object (i.e. do not change the orbital energy), therefore they are not efficient in removing debris from space. Actually, lunisolar perturbation, coupled with non-gravitational perturbations, may play a role in speeding the orbital decay of certain classes of highly eccentric orbits causing oscillations of the perigee altitude. The non-gravitational perturbations important for the space debris evolution are mainly the solar radiation pressure and the atmospheric drag (Milani et al. 1987). The latter is the most important, since it subtracts energy from an orbiting object causing its decay into the atmosphere; it represents, therefore, the main sink process. Unfortunately, the atmosphere density is decreasing exponentially with the altitude, so that this perturbation is efficient only up to about 800 km above the surface of the Earth. Above this level the air drag takes several hundreds of years to remove a typical satellite from orbit.

Another "non-natural" way to remove objects from space is the de-orbiting of the spacecraft after they completed their mission; we will discuss this issue in the following.

Since the early '90s a large mathematical model, and the related software package, have been developed in Pisa to study the long term evolution of the space debris population. In this package, named Semi Deterministic Model (SDM), the above mentioned source and sink mechanisms are modeled and the actual orbital evolution of all the larger objects produced are followed by means of an *ad-hoc* fast orbit propagator (Rossi et al. 1998).

In a typical simulation campaign, a standard scenario of the future evolution, assuming the "business-as-usual" continuation of space activities, is compared with a number of other scenarios where different physical models are used. The reference scenario is characterized by a launch activity deduced from the traffic observed over the last five years (1999-2003), adjusted by taking into account the phasing out of obsolete launchers and the introduction of new rocket families, with different hardware and mission characteristics. Mission related objects are released according to the current practices and no de-orbiting or re-orbiting of spacecraft and upper stages is performed at the End Of Life (EOF). The explosion statistics is based over the last 5 years (1999-2003) events, with an average of 2.4 explosions/year. This low value is due to the introduction of explosion prevention measures on several classes of old and new upper stages systems, such as the passivation of upper stages after burn by venting of the residual fuel. The progressive adoption of these mitigation measures by most of the launchers should lead to a stop of in-orbit explosions even if only in a few decades, due to the large number of old upper stages, left in orbit in the past and still prone to explode. As far as the production of slag is concerned, a minimum use of SRM is envisaged, based on current and planned practices (the transition to new launchers and larger commercial spacecraft is reducing considerably the reliance on such propulsion

systems). Two solid rocket motor firings are simulated for each GPS mission (perigee and apogee burns), and one of them is considered as well for each Chinese rocket Long March 3 GEO injection.

Together with the one just described, a number of other scenarios, where various mitigation measures are progressively undertaken, have been simulated. The most effective and viable mitigation measure discussed at the international level seems to be the re-orbiting of spacecraft at the end of their operative lifetime. In principle, the best solution would be to maneuver the spacecraft directly to a fiery reentry into the atmosphere just after the EOL. Nonetheless this maneuver proves to be often too demanding in terms of fuel consumption and, therefore, not acceptable by the satellite owners and operators. Hence, a delayed re-entry has been proposed: the spacecraft is initially maneuvered to a lower orbit from where it slowly decays, under the effect of the air drag, in a given number of years. Finding the best residual lifetime, taking into account the effect on the environment and the operative constraints, is one of the tasks of our long term simulations. Sometimes, anyway, even a delayed re-entry appears too expensive in terms of maneuver budget to be performed (Rossi 2002). This is the case of spacecraft having perigee above about 1400 km. For these particular cases the adoption of a long term "graveyard" orbit above the most crowded zones of LEO (i.e. above about 2000 km) have been proposed. The effectiveness of this solution has also been tested, though the hazards related to the adoption of such a mixed policy, due to the accumulation of objects in the storage zone, must be stressed.

In the first mitigation scenario (MIT_1), first the MRO are no more released starting from the year 2020, then the re-orbiting of spacecraft at EOL is performed. In particular, the GEO satellites are reorbited at EOL to a circular graveyard orbit about 300 km (depending on the actual area over mass of the satellite) above GEO, according to the recommendation of the International Advisory Debris Committee (IADC). Starting from the year 2010, all the spacecraft with $h_p < 1400$ km, or in high eccentricity orbits crossing the LEO region, are maneuvered to orbits with a residual lifetime $T_{\rm res} = 25$ years. The spacecraft with perigee height $h_p \geq 1400$ km are re-orbited in a super-LEO storage zone above 2000 km (with a width of 100 km). Concerning the upper stages, starting always from the year 2010, all those with perigee height $h_p \geq 1400$ km are left where they are, while those with $h_p < 1400$ km, or in high eccentricity orbits crossing the LEO region, are immediately de-orbited at EOL. The second mitigation scenario (MIT_2) repeats the previous one, but in this case $T_{\rm res} = 0$ years, i.e. the spacecraft with $h_p < 1400$ km, or in high eccentricity orbits crossing the LEO region, are immediately de-orbited at EOL.

Fig. 7 shows the number of objects larger than 1 cm as a function of time, between 0 and 40 000 km of altitude. In the reference scenario, an almost linear growth is observed in the first 20-30 years. This growth is sustained by the remaining on-orbit explosions and by a progressively larger number of collisions. After 2030, collisions remain the only substantial source of centimetre sized objects and a more than linear pace takes place, leading to a number of objects, after 100 years, more than twice the initial population.

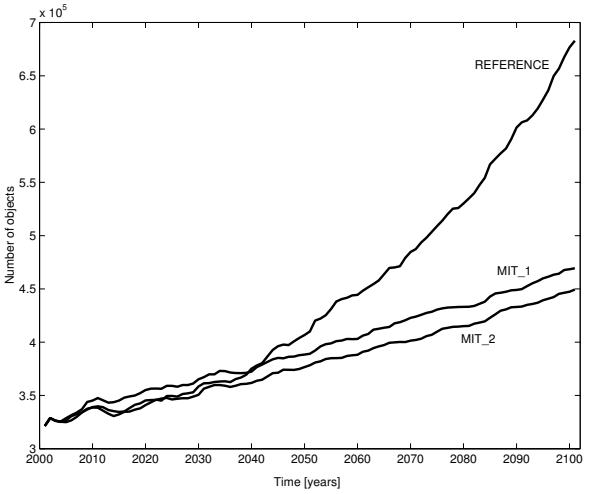


**Fig. 7.** *Number of objects with diameter larger than 1 cm, between 0 and* 40 000 *km.*

Fig. 8 shows the number of objects larger than 10 cm in LEO. The initial growth rate levels off after 2020 due the cessation of most of the on-orbit explosions and the growth rate never returns to the values experienced in the first 10-20 years, even though the absolute increase is still about a factor 2 in one century for the reference scenario.

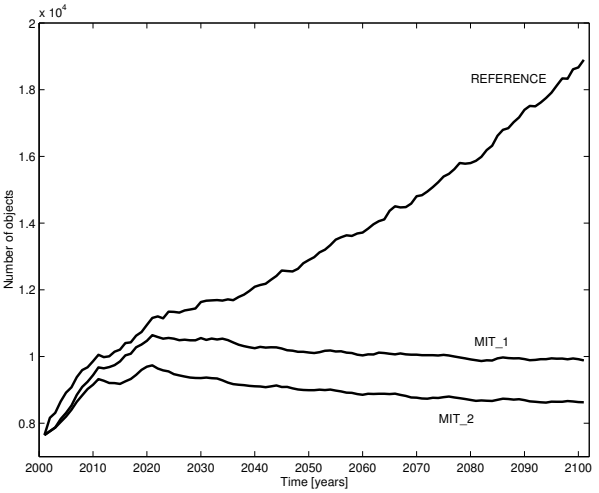


**Fig. 8.** *Number of objects with diameter larger than 10 cm, in LEO.*

Fig. 9 shows a breakdown of the objects larger than 10 cm generated during the simulation timespan (for the reference case) according to the different sources. Note the non-linear growth rate of the collision fragments as opposed to the linear trend of the launch generated objects.

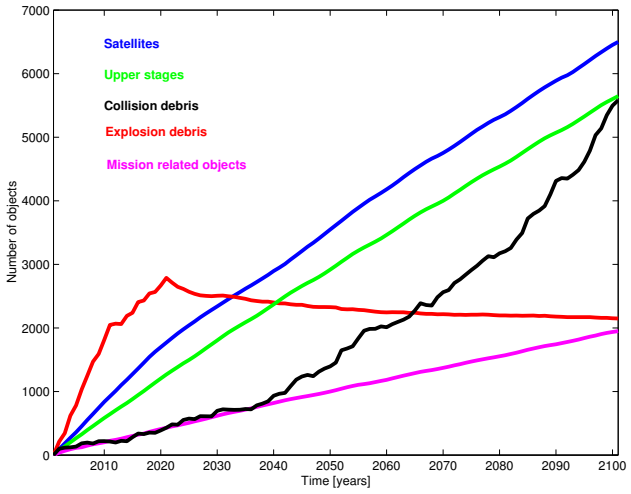


**Fig. 9.** *Breakdown, according to the different source mechanisms, of the number of objects, with diameter larger than 10 cm in the whole altitude range, generated during the simulation time span (reference case).*

The population of the objects larger than 1 m is dominated by the intact spacecraft and upper stages; in the reference scenario, these objects display a linear growth as the result of the net accumulation due to new launches in the considered time span.

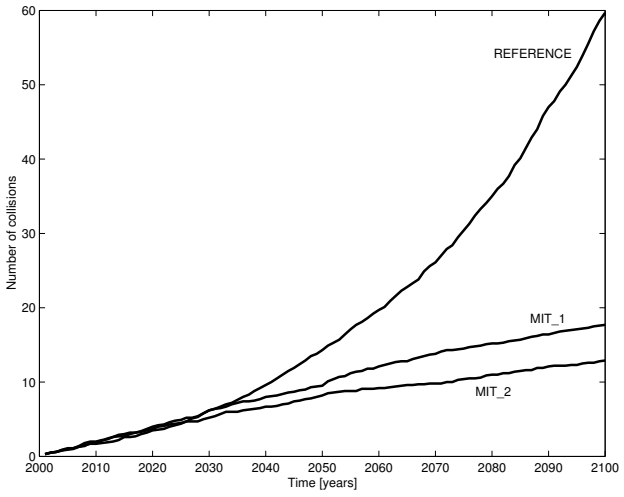


**Fig. 10.** *Number of catastrophic collisions in LEO.*

The danger posed by the growth of small and large debris, observed in the business-as-usual scenario, becomes apparent when looking at Fig. 10, where the cumulative number of catastrophic collisions in LEO is displayed. In the reference scenario there is a progressive, more than linear rise of the yearly number of catastrophic collisions. In some studies, with slightly less optimistic scenarios (i.e., less mitigation measures assumed in the business-as-usual definition), even a kind of collisional cascade has been observed in selected altitude regions (Rossi et al. 1994, Cordelli et al. 1998).

In Fig. 7 and Fig. 8 the effect of the mitigation measures (MIT_1 and MIT_2 curves) are shown in comparison with the reference case. The measures seem to be able to maintain approximately stable the growth of centimetre sized debris, with a moderate linear trend. Moreover, the adoption of a combination of re-orbiting and de-orbiting at the EOL is able to stabilize the population of objects larger than 10 cm and 1 m in LEO, and even lead to slightly decreasing trends. Another relevant result is that the two mitigation scenarios display very similar results, not only in terms of numbers of particles (with a difference of about 10 % for objects larger than 10 cm) but also, more importantly, in the trend of the growth.

These conclusions are also supported by the cumulative number of catastrophic collisions in LEO (Fig. 10). In the mitigation scenarios, the collision rate remains approximately constant, differring by a factor 3 with respect to the reference case.It is worth remembering that, due to the typical impact velocities in LEO, the fragmentation of a satellite requires a projectile larger than about 10 cm; therefore the differences seen in Fig. 8 somehow translate into Fig. 10.

In summary, the mitigation scenarios simulated seem adequately effective in mitigating over the long-term the LEO debris environment with the current launch activity. These results suggest that the use of disposal orbits might be the solution to adopt in the near future to stabilize the debris environment and to guarantee the continued exploitation of the circumterrestrial space. The slight difference between the two mitigated cases, together with the savings in propellant obtained with the less demanding maneuvers required by the MIT_1 scenario, confirm the fact that a *25-year rule* can be safely adopted to control the space debris proliferation.

It is worth noting that the results presented here were obtained by using one of the few long term evolution models developed worldwide. The adoption of a different model might lead to slightly different conclusions. On the other hand, a recent comparison of the results of three of these codes (SDM and two analogous software developed at NASA and ESA) in the simulation of a standard scenario, showed a very good agreement in the results, within the error bars of the results of each model (Rossi et al. 2005).

## 6. CONCLUSIONS

The space agencies and the satellite operators came to realize the urgency of the space debris issue. As shown by the simulations in Section 5, it is clear to all the people in the field that the situation cannot go on as business-as-usual and that some mitigation measures must be undertaken in the future space activities. More difficult is, as usual, to spread this message outside the space debris field of study and to devise common strategies to mitigate and solve

the problem. Currently the most favored *mitigation measures* include:

i change of the spacecraft design to prevent the release of mission related debris;

ii prevent on-orbit explosions: this includes venting the upper stages of the residual fuel to avoid over-pressurization and discharging any power system on board after the end of the operational life;

iii de-orbit all the upper stages and the satellites at the end-of-life (either direct or delayed re-entry). If the original orbit is such that a de-orbiting maneuver is too demanding in terms of propellant, than a re-orbiting to a storage orbit above the operative one could be envisaged. The latter might be a short-term solution, that could be abandoned whenever other propulsion methods (e.g., low thrust systems or even electrodynamics tethers) become commonly available on the spacecrafts for de-orbiting purposes.

The main international committee established to study and face the space debris issue is the Inter-Agency Debris Coordination Committee (IADC) (see the web page: `http://www.iadc-online.org`) that periodically gathers the representatives of all the main space agencies to share the results of the researches on the different aspects of the field. Though the IADC has no power to legislate or enforce any rule, its role is of paramount importance in issuing recommendations that can be passed to higher political levels within each country. The IADC is also in contact with the United Nations Committee on the Peaceful Uses of Outer Space (COPUOS), that issued a Technical Report on Space Debris available at `http://www.oosa.unvienna.org/isis/pub/sdtechrep1/index.html`.

Notwithstanding the wealth of theoretical results and the efforts of these organizations, it must be noted that the actual implementation of the mitigation measures sometimes may collide with technical, political or economical reasons that can slow down and reduce their efficiency. As an example, in the last few years only about 10 % of the GEO satellites have followed the de-orbiting procedures recommended by the IADC. In fact the operators often tend to privilege the immediate return of a few more months of operations, performed with the fuel that should be used for the de-orbiting maneuvers, as opposed to the long term benefit of all the space environment.

*Acknowledgements* – Part of the work presented in this paper was done in the framework of the Contract ESOC No. 15857/D/HK(SC).

REFERENCES

Alby, F., Lansard, E. and Michal, T.: 1997, *Second European Conference on Space Debris*, Proceedings ESA SP-393 (Darmstadt), 589.

Cordelli, A., Rossi, A. and Farinella, P.: 1998, *Planetary and Space Science*, **46**, 691.

Flury, W., Massart, A., Schildknecht, T., Hugentobler, U., Kuusela, J., Sodnik, Z.: 2000, ESA Bulletin, **104**, 92.

Foster, J., Krisko, P., Matney, M. and Stansbery, E.: 2003, *$54^{th}$ International Astronautical Congress*, Paper IAC-03-IAA.5.2.02 (Brehmen, Germany).

Goldstein, R.M., Goldstein, S.J. and Kessler, D.J.: 1998, *Planetary and Space Science*, **46**, 1007.

Jackson, A., P. Eichler, Potter, R., Reynolds, A. and Johnson, N.: 1997, *Second European Conference on Space Debris*, Proceedings ESA SP-393 (Darmstadt), 279.

Kessler, D.J. and Cour–Palais, B.G.: 1978, *J. Geophys. Res.*, **83**, 2637.

K., Klinkrad, H., Krag, H., Martin, C., Sdunnus, H., Walker, R., Wegener, P.: 2004, *Advances in Space Research*, **34**, 959.

Liou, J.-C., Matney, M.J., Anz-Meador, P.D., Kessler, D., Jansen, M. and Theall, R.: 2002, *NASA/TP-2002-210780.*

Milani, A., Nobili, A. and Farinella, P.: 1987, Non gravitational perturbations and satellite geodesy, Adam Hilger Ltd., Bristol and Boston.

Öpik, E.J.: 1976 *Interplanetary Encounters*, Elsevier, New York, USA.

Petit, J.–M. and Farinella, P.: 1993, *Celest. Mech. Dyn. Astron.*, **57**, 1.

Rossi, A. and Farinella, P.: 1992, *ESA Journal*, **16**, 339.

Rossi, A., Cordelli, A. Farinella, P. and Anselmo, L.: 1994, *J. Geophys. Res.*, **99**, No. E11, 23 195.

Rossi, A., Anselmo, L., Cordelli, A., Farinella, P. and Pardini, C.: 1998, *Planetary and Space Science*, **46**, 1583.

Rossi, A., Valsecchi, G.B. and Farinella, P.: 1999, *Nature*, **399**, 743.

Rossi A. and Valsecchi, G.B.: 2001, *Second International Workshop on : Satellite Constellations and Formation flying*, February 19-20, 2001, Haifa, Israel.

Rossi, A.: 2002 *Journal of Spacecraft and Rockets*, **39**, No. 4, 540.

Rossi A., Valsecchi, G.B. and and Perozzi, E.: 2004a, *Journal of Astronautical Science*, in press.

Rossi, A., Anselmo, L., Pardini, C., Valsecchi, G.B. and Jehn, R.: 2004b, *$55^{th}$ International Astronautical Congress*, Paper IAC-04-IAA.5.12.1.06 (Vancouver, Canada).

Rossi, A., Liou, J.C., Martin, C. and Lewis, H.: 2005, LEO Modelling Comparison, *$23^{rd}$ IADC Plenary Meeting*, ESOC, Darmstadt, Germany, 21–22 April 2005.

Schildknecht, T., Musci, R., Ploner, M., Beutler, G., Flury, W., Kuusela, J., de Leon Cruz, J., de Fatima Dominguez Palmerod, L.: 2004, *Advances in Space Research*, **34**, 901.

Valsecchi, G.B., Rossi, A. and Farinella, P.: 1999, *Space Debris*, **1**, 143.

Valsecchi, G.B. and Rossi, A. : 2002, *Celest. Mech. Dyn. Astron.*, **83**, 63.

# СВЕМИРСКИ ОТПАД У ЗЕМЉИНОЈ ОРБИТИ

**A. Rossi**

*ISTI–CNR*
*Via Moruzzi 1, 56124 Pisa, Italy*

UDK 521.1 : 523.31
*Прегледни рад по позиву*

Популација свемирског отпада слична је астероидном појасу, јер се и у њој догађају међусобни судари на великим релативним брзинама, који утичу на еволуцију расподеле тела по величини. У овом тренутку више од 10000 комада вештачки створеног отпада пречника изнад 10 cm (а више од 300000 комада пречника већег од 1 cm) кружи око Земље и сви се они прате и изучавају помоћу велике мреже сензора распоређене по читавој Земљи. Популацију свемирског отпада чине многе различите врсте објеката насталих на разне начине, од високо енергетских распада великих свемирских летелица, до споре дифузије течног метала. Удар неког комада свемирског отпада представља данас ризик са којим се свака нова свемирска мисија мора суочити, а који се може проценити помоћу одређених ad-hoc поступака. Еволуција целокупне популације свемирског отпада изучава се помоћу компјутерских модела који симулирају све познате механизме настанка и нестанка отпада. Један од ових програма описан је у овом раду, као и резултујуће могуће еволуције популације отпада и окружења у наредних 100 година, које се предвиђају на основу различитих сценарија будућег саобраћаја. Такође се указује и на мере које је могуће предузети да би се спречио и задржао под контролом будући раст популације орбиталног отпада.